Influence of Metal Deposition on Electrochemical Impedance Spectra of Porous GaP and GaN Semiconductors

Liana ANICAI[1], Florentina GOLGOVICI[1], Eduard MONAICO[2], Veaceslav URSAKI[3*] Mariana PRODANA[1], Marius ENACHESCU[1], Ion TIGINYANU[2,3]
[1]*Center for Surface Science and NanoTechnology, University Politehnica of Bucharest*
[2]*National Center for Material Study and Testing, Technical University of Moldova*
[3]*Institute of Electronic Engineering and Nanotechnologies, Academy of Sciences of Moldova*
**ursaki@yahoo.com*

***Abstract* — A comparative analysis of electrochemical impedance spectroscopy (EIS) characterization is performed in porous GaN and GaP templates with and without metal nanostructured layers deposited by pulsed electroplating. The porous semiconductor templates are produced by electrochemical etching of bulk substrates. The EIS data are interpreted in terms of electrical equivalent circuits (EECs) deduced by fitting the experimental data from Nyquist plots. It is found that the EIS data of porous electrodes without electroplating are best fitted with EECs with both the charge transfer and mass transfer components of the Faradaic impedance, while electroplating reduces the importance of the mass transport component, i. e. of the Warburg impedance, associated with diffusion, in favor of the charge transport phenomena.**

***Index Terms* — Porous semiconductor, electroplating, electrochemical impedance spectroscopy, mass transfer.**

I. INTRODUCTION

Electrochemical impedance spectroscopy (EIS) is known as a powerful tool for characterization of electrode processes and complex interfaces, for investigating the mechanisms of electrochemical reactions, for measuring the dielectric and transport properties of materials, for investigating the coatings and corrosion processes, for dye-sensitized solar cells, Li-ion batteries, fuel cells, and biosensors characterization [1-9]. EIS is a technique based on the analysis of the linear response of a system perturbed by a small sinusoidal potential or current and the experimental data are often fitted with electrical equivalent circuits (EECs), which provide information about the interface, its structure and processes taking place there.

EIS is particularly useful to investigate the anodization processes by giving insight into the fundamentals of the charge-transfer and dissolution processes, and by providing information about the influence of nanopore dimensions on the electrochemical properties of porous materials [10,11].

Porous III-V semiconductor compounds have been widely explored due to their potential applications in the field of electronics and photonics [12,13]. Particularly, porous GaP layers and free-standing membranes proved to be excellent for studying the peculiarities inherent to porous III-V semiconductor compounds when preparing porous structures with controlled morphology by electrochemical etching. It was also recently shown that nanoporous GaN with a controlled porosity through the applied anodic voltage can be produced by electrochemical etching [14].

On the other hand, the deposition of metal nanoparticles on semiconductor substrates and matrices is of great importance for controlled growth of semiconductor nanostructures, enhanced solar energy absorption in thin-film photovoltaic structures, fabrication of plasmonic nanoarchitectures for surface enhanced spectroscopy etc.

Therefore, the goal of this paper is to investigate the influence of metal nanoparticles deposition into porous GaN and GaP layers upon their electrochemical impedance characteristics in terms of EECs.

II. DESCRIPTION OF TECHNOLOGICAL PROCEDURES

Crystalline 500-μm thick n-GaP(111) substrates with the free electron concentration of $2x10^{17}$ cm^{-3} supplied by CrysTec GmbH were subjected to anodic etching in 500 ml of 1 M HBr aqueous solution at 25 ^oC to fabricate porous layers as described elsewhere [15].

Wurtzite-phase 2-inch diameter HVPE-grown n-GaN substrates of (0001)-orientation with thickness of 300 μm, with the virgin Ga-face and the polished N-face from SAINT-GOBAIN Crystals were electrochemically etched in 0.3M HNO_3 aqueous electrolyte in a two-electrode cell where the sample served as working electrode. An anodic voltage of +25 V was applied to the sample for 20 minutes.

Electroplating of Au or Ag was performed at 25^oC in a common two-electrode plating cell with commercially available gold or silver baths (DODUCO) where the porous sample served as working electrode, while a platinum wire was used as counter electrode. A pulsed voltage with pulse duration of 50 ms and a cathodic voltage of - 25 V was applied between the two electrodes to electrochemically reduce the metal species on the surface of the samples

being in contact with the electrolyte. After each pulse, a delay time as long as one second was kept. The solution was magnetically stirred to provide appropriate conditions for the recovery of the ion concentration in the electrolyte.

Fig. 1a shows the SEM image taken from the N-face of the GaN sample after anodic etching. Quasi-circular porous regions, sometimes resembling hexagonal shape, are seen in the bright areas of the SEM image. Alternation of regions with high and low degrees of porosity was attributed to the spatial modulation of the electrical conductivity in the HVPE-grown samples, as also evidenced by KPFM techniques [16]. It is known that the degree of porosity of electrochemically etched samples depends upon the electrical conductivity, samples with higher electrical conductivity being characterized by higher degree of porosity.

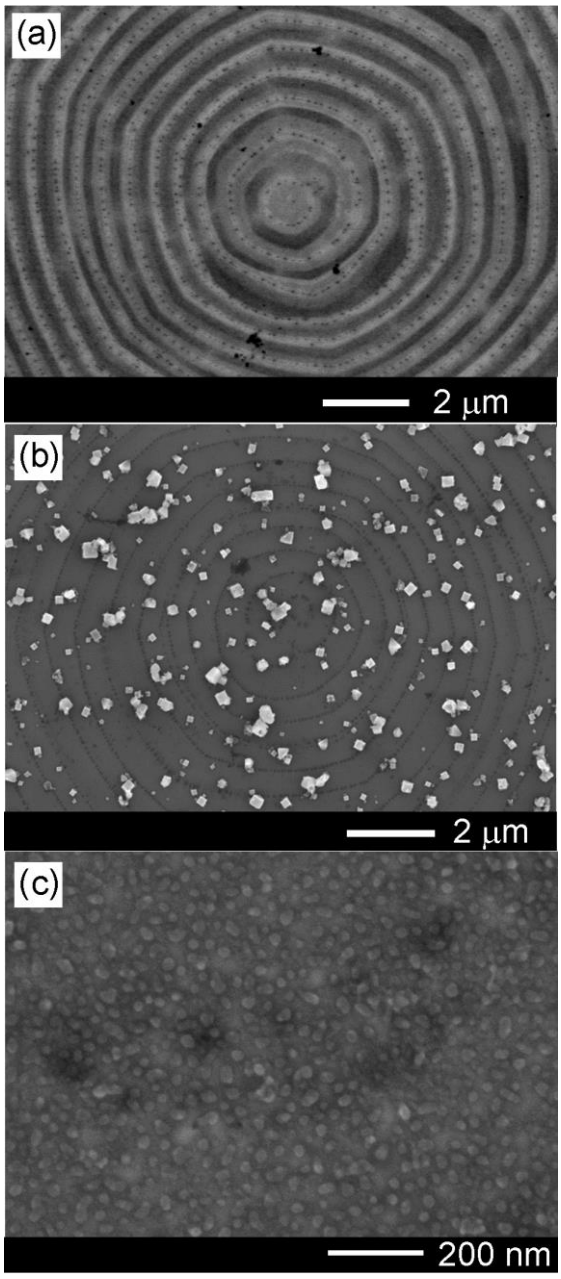

Fig. 1. (a) SEM view of the N-face of the GaN sample after anodic etching. (b) SEM view of the sample after Au deposition. (c) Enlarged SEM view of the sample after Ag deposition.

One can see from Fig. 1b that Au electroplating results in a non-uniform deposition of larger metal formations, while a uniform layer of Ag nanoparticles is deposited after Ag electroplating during 1 minute on the porous GaN sample (Fig. 1c).

Fig. 2a illustrates the SEM image taken from a porous GaP sample fabricated under potentiostatic anodic etching with an applied voltage of 10 V with a subsequent pulsed electrodeposition of Ag for 1 min.. The enlarged view of the etched sample without metal deposition reveals the formation of a complex porous structure consisting of bigger and smaller pores (Fig. 2b), while the enlarged view of the sample after electroplating suggests that the electrodeposition is non-uniform, only some regions of the porous sample being covered by Ag formations (Fig. 2c).

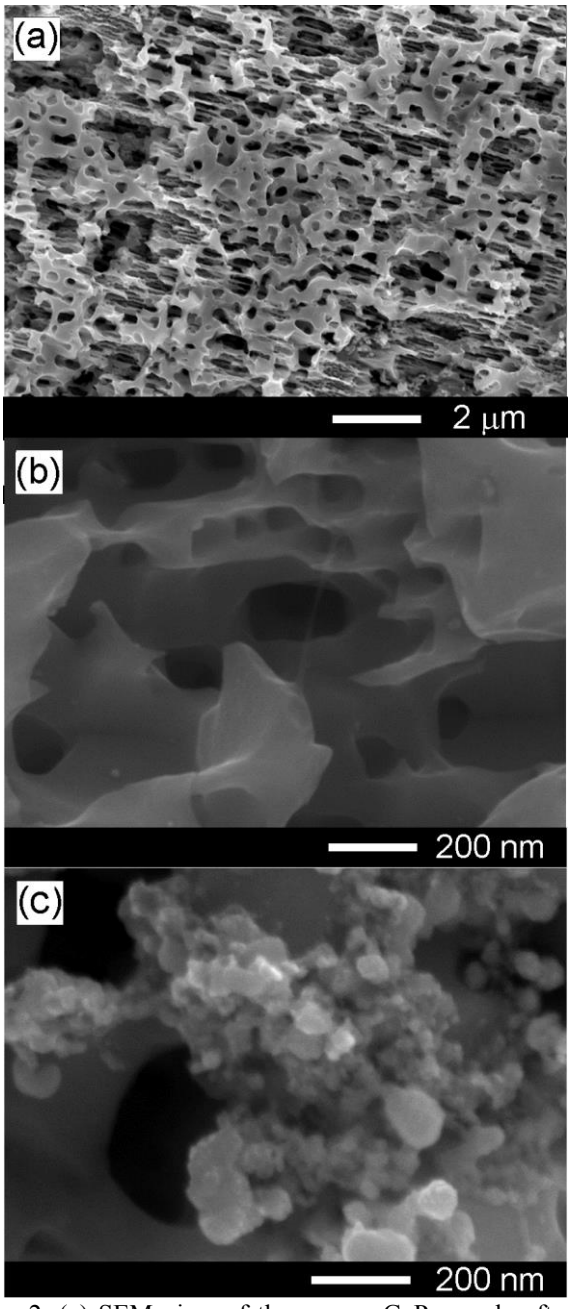

Fig. 2. (a) SEM view of the porous GaP sample after Ag deposition. (b) Enlarged SEM view of the sample without metal deposition. (c) Enlarged SEM view of the sample with Ag metal deposition.

III. Electrochemical Impedance Spectroscopy Characterization

EIS experiments have been performed in a 25 cm^3 cell at room temperature in stationary conditions with a Pt counter electrode and an Ag/AgCl reference electrode using a PARSAT 4000 instrument and an AUTOLAB electrochemical system. A Na_2SO_4 0.5M, pH = 6.5 solution in aerated conditions was used for the electrochemical investigations. Measurements have been conducted with a 10 mV sinusoidal signal in a frequency range of 10^6 Hz ÷ 1 Hz. A Zview 2.9b software (Scribner Associates Inc.) was used for experimental data fitting.

The samples were mounted on a Cu conducting tape, and the working surface in contact with the electrolyte was defined by a mask. Fig. 3 presents the recorded EIS for different GaN samples.

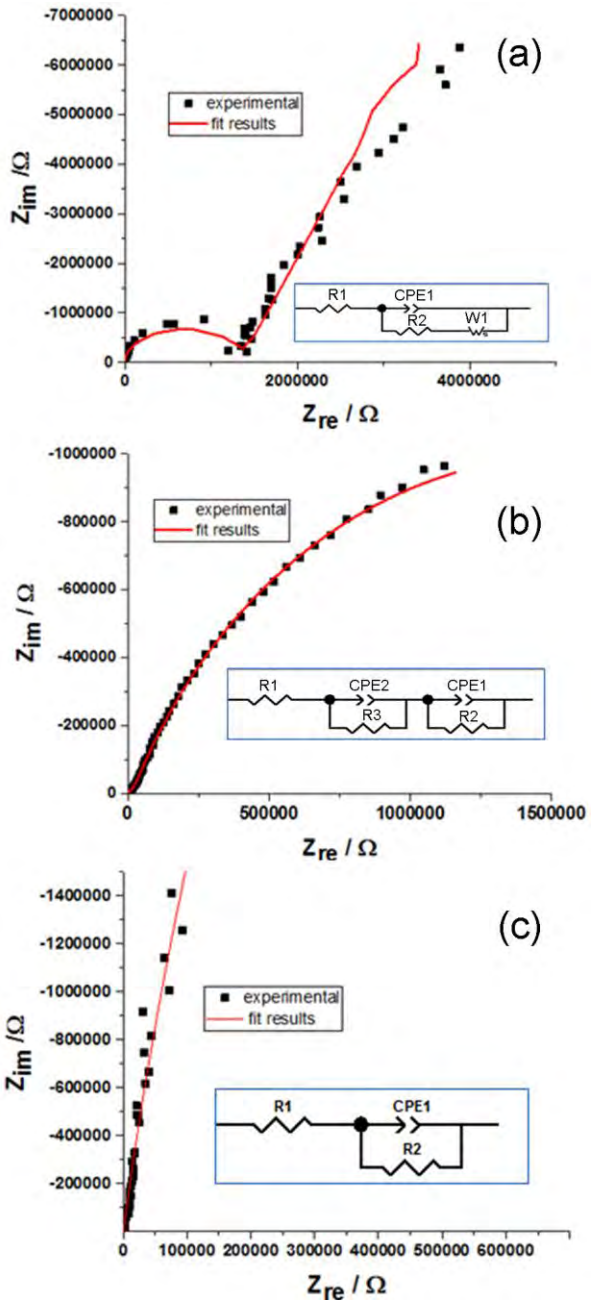

Fig. 3. EIS Nyquist plot for a porous GaN sample (a), a porous sample with Au electroplating (b), and a porous sample with Ag electroplating (c). Inset are EECs.

The results of EIS are interpreted in terms of EECs deduced by fitting the experimental data. The Nyquist plot for the GaN porous sample measured at open circuit potential OCP = 0.17 V *vs* Ag/AgCl reference electrode shows a straight line with a slope of 45° at low frequencies and a semicircle at high frequencies. It is known that the Warburg impedance with the phase angle of 45° appears as a straight line in the Nyquist plot. Therefore, a classical Randles-type EEC was proposed for fitting the experimental data, consisting of the solution resistance R1 in series with parallel connection of the double layer (DL) capacitance at the semiconductor/electrolyte interface and the Faradaic impedance composed of the charge transfer resistance R2 and the Warburg impedance W1 associated with mass transfer phenomena. We used a "constant phase element" (CPE) instead of the capacitance for better data fitting. A CPE is described mathematically as $Z_{CPE} = A/(j\omega)^n$, where A and *n* are empirical constants.

The values of the EEC components for the porous GaN sample obtained as result of experimental data fitting are presented in Table 1.

TABLE I. THE EEC COMPONENTS FOR THE POROUS GAN SAMPLE

R1, Ω	CPE1		R2, Ω	R_W, Ω
	C, $\Omega^{-1}.s^n$	*n*		
$5.5\cdot10^{-7}$	$1.2\cdot10^{-10}$	0.99	$1.4\cdot10^{6}$	$4.7\cdot10^{7}$

The value of the *n* coefficient close to 1 is indicative of the capacitive nature of the CPE, which corresponds to the capacitance of the DL. It is known that the CPE corresponds to a capacitor, resistor, and inductor, respectively, when *n* is 1, 0, and -1.

The Nyquist plot for the GaN porous sample with Au electroplating measured at OCP = 0.05 V presented in Fig. 3b suggests the presence of two time constants. An EEC composed of the electrolyte resistance R1 in series with two CPE-R combinations was proposed for fitting the experimental data. The fitted values of the components of this EEC are summarized in Table 2.

TABLE 2. THE EEC COMPONENTS FOR THE POROUS GAN SAMPLE WITH AU ELECTROPLATING

R1, Ω	CPE2		R3, Ω	CPE1		R2, Ω
	C, $\Omega^{-1}.s^n$	*n*		*C*, $\Omega^{-1}.s^n$	*n*	
$5.5\cdot10^{-7}$	$1.2\cdot10^{-7}$	0.73	$3.1\cdot10^{6}$	$4.4\cdot10^{-8}$	0.73	$1.7\cdot10^{4}$

One can suppose that the presence of two time constants and two CPE-R combinations for this sample is related to the fact that the surface of the porous GaN sample is only partially covered by Au formations. One can suggest that R3 is related to the charge transfer at the porous GaN/electrolyte interface, while the R2 is associated with charge transfer at the surface covered by Au metal. Note that R3 has the same order of magnitude as R2 from Table 1, while the value of R2 is two orders of magnitude lower. One should also notice that the value of *n* is substantially different from 1 for both CPE-R circuits, which means that CPE can not be treated as the capacitance of the DL in this case.

In contrast to the GaN sample with Au electroplating, the EIS data for the sample with Ag electroplating measured at OCP = -0.2 V and presented in Fig. 3c are well fitted by a simpler EEC consisting of the electrolyte resistance R1 in

series with one CPE-R combination. The R2 in this circuit can be treated as charge transfer resistance, while CPE - as the capacitance of the DL, since the value of the *n* coefficient is close to 1, as shown in Table 3. The difference between these two samples is explained by the observation that the sample with Ag electroplating is covered by a more uniform layer of Ag nanoparticles as shown in Fig. 1c, in contrast to the sample with Au electroplating.

TABLE 3. THE EEC COMPONENTS FOR THE POROUS GAN SAMPLE WITH AG ELECTROPLATING

R1, Ω	CPE		R2, Ω
	$C, \Omega^{-1}.s^n$	*n*	
$1.7 \cdot 10^{-6}$	$2.0 \cdot 10^{-10}$	0.97	$1.0 \cdot 10^{8}$

The results of EIS measurements performed on GaP samples are shown in Fig. 4.

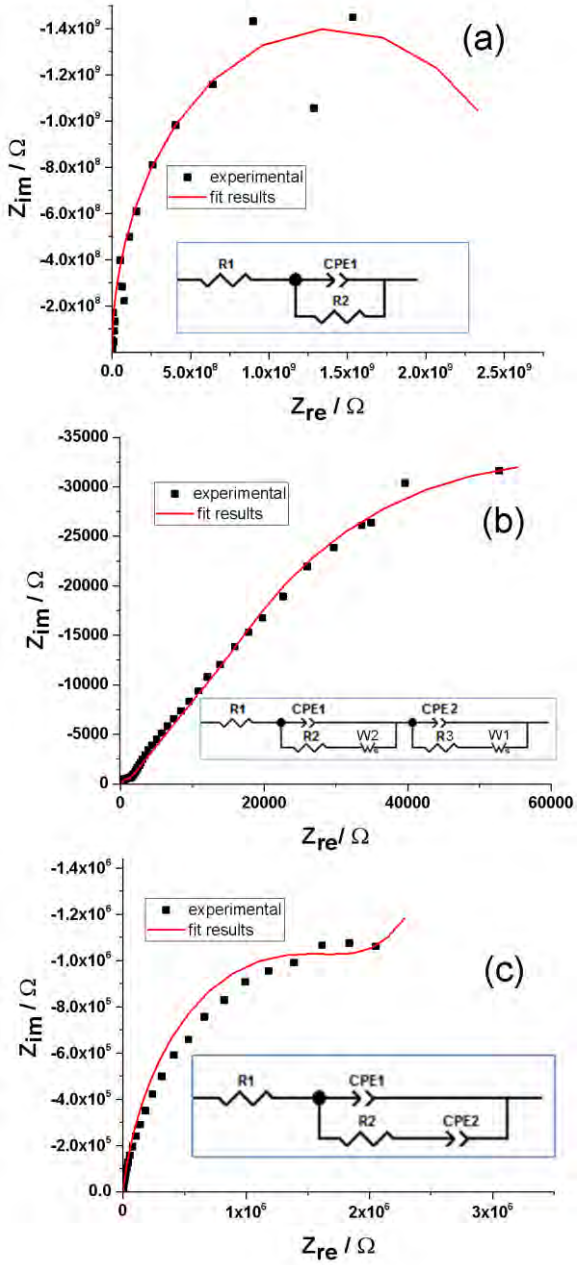

Fig. 4. EIS Nyquist plot for a bulk GaP sample (a), a porous sample (b), and a porous sample with Ag electroplating (c). Inset are the proposed EECs to fit the experimental data.

Similarly to the porous GaN sample covered by a uniform layer of Ag nanoparticles, the EIS data for the bulk GaP sample as shown in Fig. 4a are well fitted by a simple EEC consisting of the electrolyte resistance R1 in series with parallel connection of the DL capacitance at the bulk semiconductor/electrolyte interface and the charge transfer resistance R2. The constant phase element CPE1 can again be treated as the DL capacitance, since the value of the *n* coefficient is close to 1, as shown in Table 4.

TABLE 4. THE EEC COMPONENTS FOR THE BULK GAP SAMPLE

R1, Ω	CPE1		R2, Ω
	$C, \Omega^{-1}.s^n$	*n*	
11.5	$3.5 \cdot 10^{-10}$	0.96	$3.1 \cdot 10^{9}$

The recorded EIS as Nyquist plot for the porous GaP illustrated in Fig. 4b is relatively similar to that from Fig. 3b for the porous GaN with Au electroplating. In order to demonstrate the presence of two time constants, Fig. 5 shows the Nyquist plot in the high frequency region of the porous GaP. The presence of another semicircle is noticed in this graph, suggesting the presence of two time constants. A similar behavior was noticed for the spectrum in Fig. 3b (not shown here).

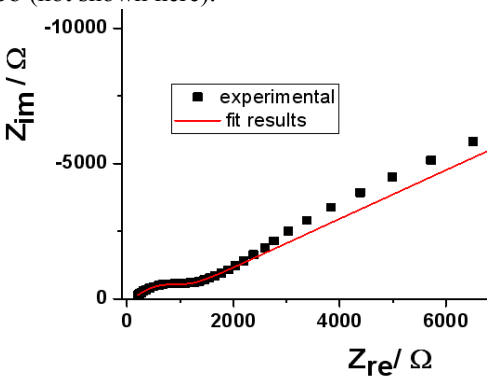

Fig. 5. EIS Nyquist plot for the porous GaP sample in the high frequency region

Therefore, the EEC for the porous GaP sample is composed of the electrolyte resistance R1 in series with two CPE-Faradaic impedance combinations. However, the Faradaic components are composed of both charge transfer resistance (R2 and R3) and Warburg impedance (W2 and W1), in contrast to the porous GaN with Au electroplating, where the EIS data were well fitted with only the charge transfer resistance (R2 and R3) components.

The values of the EEC components for the porous GaP sample obtained as result of experimental data fitting are summarized in Table 5.

TABLE 5. THE EEC COMPONENTS FOR THE POROUS GAP SAMPLE

R1, Ω	CPE1		R2, Ω	R_{W2}, Ω	CPE2		R3, Ω	R_{W1}, Ω
	$C, \Omega^{-1}.s^n$	*n*			$C, \Omega^{-1}.s^n$	*n*		
20	$3.9 \cdot 10^{-8}$	1	540	$2.3 \cdot 10^{4}$	$1.1 \cdot 10^{-5}$	0.43	600	$1.5 \cdot 10^{5}$

While the existence of two time constants for the porous GaN with Au electroplating was suggested to be related to the presence of porous sample regions covered and uncovered by Au metal particles, the existence of two time constants for the porous GaP sample can be explained by the complex morphology consisting of bigger and smaller pores as discussed in the previous section with relation to the Fig. 2b.

The two different Faradaic components of the porous GaP electrode can be explained by differences in charge transfer processes and diffusion processes of species from the electrolyte in small and large pores.

A comparison of EECs for porous samples with and without metal electroplating suggests that the Faradaic impedance of electrodes with metal electroplating is dominated by the charge transfer components, while both charge transfer and mass transfer phenomena are characteristic for porous electrodes without metal electroplating.

Finally, the EIS data of the porous GaP sample with Ag electroplating were fitted involving an EEC consisting of the electrolyte resistance R1 in series with a combination representing a parallel connection of the CPE1 in one branch and a series connection of the R2 and CPE2 in another branch, and the determined values are presented in Table 6. However, one should mention that fitting for this sample is not so perfect, and the interpretation of data is not so straightforward. First of all, both the CPE are not pure capacitive (the *n* values are quite different from 1). That means that CPE2 could be replaced by aWarburg impedance. Actually, the Warburg impedance can be interpreted as a CPE with the value of *n* equal to 0.5. It was previously shown that a CPE element can be substituted in some cases by a Warburg impedance. The complexity of this sample is argued by the presence of pores with different sizes, and by a complex morphology and non-uniformity of the Ag electroplating as deduced from Fig.1c.

TABLE 6. THE EEC COMPONENTS FOR THE POROUS GAP SAMPLE WITH AG ELECTROPLATING

R1, Ω	**CPE1**		**R2, Ω**	**CPE2**	
	***C*, $\Omega^{-1}.s^n$**	***n***		***C*, $\Omega^{-1}.s^n$**	***n***
280	$3.4 \cdot 10^{-8}$	0.86	$2.3 \cdot 10^{6}$	$5.3 \cdot 10^{-7}$	0.7

IV. CONCLUSION

The results of this study suggest that the deposition of metal nanostructure layers in porous semiconductor templates modifies the electrical equivalent circuits used for fitting the EIS data mostly by reducing the importance of mass transfer components of the Faradaic impedance. More uniform electrodeposited Au and Ag nanostructures may contribute to a better EIS response.

ACKNOWLEDGMENTS

This work was supported financially by Academy of Sciences of Moldova under the grant No. 16.80013.5007.08/RO, by Romanian Ministry of Education and Scientific Research and by Executive Agency for Higher Education, Research, Development and Innovation, under Projects PCCA 66/2014 and ENIAC 04/2014.

REFERENCES

[1] D. D. Macdonald, "Reflections on the history of electrochemical impedance spectroscopy," Electrochimica Acta, vol. 51, pp. 1376, 2006.

[2] D. D. Macdonald, Transient Techniques in Electrochmistry. Plenum Press, New York, 1977

[3] J. R. Macdonald (Ed), Impedance Spectroscopy Emphasizing Solid Materials and Systems, Wiley/Interscience, New York, 1987.

[4] M. E. Orazem and B. Tribollet, "Electrochemical Impedance Spectroscopy", Wiley, 2008.

[5] S. Skale, V. Dolecek, M. Slemnik, "Substitution of the constant phase element by Warburg impedance for protective coatings, Corossion Sci., vol. 49, pp. 1045, 2007.

[6] Q. Wang, J. E. Moser, M. Gratzel, "Electrochemical impedance spectroscopy analysis of dye-sensitized solar cells", J. Phys. Chem. B., vol. 109, pp. 14945, 2005.

[7] J. Guo, X. Chen, C. Wang, "Carbon scaffold structured silicon anodes for lithium-ion batteries", J. Mater. Chem., vol. 20, pp. 5035, 2010.

[8] M. A. Danzer, E. P. Hofer, "Analysis of the electrochemical behaviour of polymer electrolyte fuel cells using simple impedance models", J. Power Sources, vol. 190, pp. 25, 2009.

[9] B. Y. Chang and S. M. Park, "Electrochemical Impedance Spectyroscopy", Annu. Rev. Anal. Chem., vol. 3, pp. 207, 2010.

[10] D. Vanmaekelbergh and P. C. Searson, "on the electrical impedance due to the anodic dissolution of silicon in HF solutions", J. Elecrochem. Soc., vol. 141, pp. 697, 1994.

[11] K. Kant, C. Priest, J. G. Shapter, D. Losic, "The influence of nanopore dimensions on the electrochemical properties of nanopore arrays studied by impedance spectroscopy", Sensors, vol. 14, pp. 21316, 2014.

[12] A. Sarua, J. Monecke, G. Irmer, I. M. Tiginyanu, G. Gartner, H. L. Hartnagel, "Frohlich modes in porous III-V semiconductorts", J. Phys.:Conddens. Matter, vol. 13, pp. 6687, 2001.

[13] I. Tiginyanu, E. Monaico, V. Sergentu, A. Tiron, V. Ursaki, "Metallized porous GaP templates for electronic and photonic applications", ECS J. Sol. St Sci. Technol., vol. 4, pp. P57, 2015.

[14] D. Chen, H. Xiao, J. Han, "Nanopores in GaN by electrochemical anodization in hydrofluoric acid: formation and mechanism", J. Appl. Phys., vol. 112, pp. 064303, 2012.

[15] I. Tiginyanu, E. Monaico, K. Nielsch, "Self-assembled monolayer of Au nanodotes deposited on porous semiconductor structures", ECS Electrochem. Lett., vol. 4, pp. D8, 2015.

[16] I. Tiginyanu, M. A. Stevens-Kalceff, A. Sarua et al., "Self-organized three-dimensional nanostructured architectures in bulk GaN generated by spatial modulation of doping", ECS J. Solid St. Sci. Technol., vol. 5, P218, 2016.

[17] S. Skale, V. Dolecek, M. Slemnik, "Sustitution of the constant phase element by Warburg impedance for protective coatings", Corrosion Sci., vol. 49, pp. 1045, 2007.